

Transducer based measurements of Terfenol-D material properties

Frederick T. Calkins
Alison B. Flatau

Department of Aerospace Engineering and Engineering Mechanics
Iowa State University
Ames IA 50011

ABSTRACT

Quantification of Terfenol-D material properties is not readily achieved through standard stress-strain test procedures due to the sensitivity of material properties to changes in magnetic and mechanical loads. A Terfenol-D transducer can be used to measure material properties under varied operating conditions. The development of the measurement and calculation procedures used to obtain material properties is based on the model of low signal, linear magnetostriction, linear transduction equations for a transducer, and a one degree of freedom mechanical model of the transducer. Vector impedance and admittance analysis is used to determine the transducer resonant, anti-resonant, and half power point frequencies. Using these frequencies, acceleration from an accelerometer mounted on the transducer, readily measurable transducer and Terfenol-D rod parameters (mass, length, etc.), and the calculation procedures described, pertinent material properties such as the Young's moduli, permeabilities, magnetomechanical coupling factor, and the linear coupling coefficient (d_{33}) can be determined. The subtleties of applying this theory to real world non-linear Terfenol-D operated in an transducer are addressed, including proper design and operation of a transducer to achieve circular Nyquist mobility loops. Experimental results from this method are compared with other research and the material property trends are found to be consistent.

1. BACKGROUND

One of the challenges facing magnetostrictive transducer designers is the lack of reliable material property data needed for accurate, predictive modeling. The well developed theory of electroacoustics provides a vehicle for evaluating the material properties of the magnetostrictive component of the transducer from transducer measurements. The material properties are calculated from the electroacoustic model of transduction, a linear, small signal model of magnetostriction, and a one degree of freedom mechanical model of the transducer. Material properties for specimen samples can then be measured under real world, dynamic conditions. Real world conditions implies operation of the transducer in an imperfect environment, as would be true for most engineering applications, rather than in the laboratory environment. In a transducer the Terfenol-D rod is part of the magnetic circuit; it is under a known prestress which nonetheless will vary during operation; and it may see a non-uniform magnetic field. Therefore, given the sensitivity of Terfenol-D performance to the conditions under which the transducer is operated, it is important to measure the material properties under similar conditions.

Electroacoustics theory models how a transducer converts oscillatory electric energy into mechanical or sound energy and vice versa. This model illustrates how transducer input and output measurements can be used to identify material properties of the transduction element in the transducer. This method is broadly applicable to Terfenol-D samples of various qualities, stoichiometries, laminations, and sizes.

Terfenol-D is a magnetostrictive alloy of the rare earths terbium and dysprosium with iron. In its demagnetized state the material's magnetic domains are randomly oriented and therefore it has no resultant induction at the macroscopic level. However, when a magnetic field is applied the domains deform and align with the field's direction thus resulting in a gross deformation of the material. In addition, a mechanical deformation of the material will produce a change in the orientation of the domains, changing the induction at a macroscopic level. In simple terms the application of a magnetic field forces the magnetic domains in the alloy to align themselves with the field. The domain rotation results in material strain. An AC signal applied to a transducer will cause an oscillatory strain in the Terfenol-D sample that can be used to drive an external load.

The Terfenol-D transducer in use is a broadband laboratory prototype designed to maximize output, ease of use, and reduce spurious resonances. Washers provide a mechanical prestress, which can be varied. A two inch long, quarter inch diameter Terfenol-D sample is placed inside two coils, an inner single layer pick-up coil, and a multi-layer drive coil. The drive coil

can be used to provide the AC magnetic field and a DC magnetic bias as needed. Additional magnetic bias is provided by a slit, cylindrical permanent magnet which surrounds the coils. The measurable quantities from the transducer include the current and voltage in the drive coil, a pick-up coil voltage (based on Lenz-Faraday law of magnetic induction), and the transducer output acceleration.

Early work by Moffett et al.¹ established the dependence of material properties, such as the magnetomechanical coupling k^2 , axial strain coefficient q (d_{33}), permeability at constant stress μ , and Young's Modulus at constant applied field E^H , on both prestress and magnetic bias. As later development will show, the material properties will be a function of many interrelated quantities, such as prestress, magnetic bias, drive level or amplitude of the AC applied field, and less obvious influences such as temperature, and the type of drive signal (constant current or voltage) used to obtain the AC magnetic field. Therefore, any discussion of material properties must explicitly state the conditions under which the properties have been measured. There will not be one constant value of a material property, such as permeability, that can be plugged into a model and used to achieve accurate results under all conditions. In fact, for a given set of operating conditions, two values of the material properties, such as permeability, Young's Modulus, or speed of sound, are cited in the literature. The dual values can be understood from the reaction of the material to different operating conditions. For example, the material will appear stiffer at constant magnetic induction than at constant applied magnetic field because in the former case there is not the magnetic domain rotation of the later case, resulting in a higher apparent stiffness. Therefore, two Young's Moduli, one at constant induction and one at constant applied field, are needed to describe the behavior of the material.

2. ELECTROACOUSTICS

"The science of electroacoustics is based on the experimental observation that an electrical system can be associated with a mechanical system in such a way that a unique functional relation exists between the variables that characterize the electrical system and the variables that characterize the mechanical system." This description and a thorough development of the electroacoustic theory presented here can be found in Hunt². The transduction equations from electroacoustics can describe the experimentally observed relationship between mechanical and electrical systems. These two linear equations, which will describe electromechanical coupling of a magnetostrictive transducer, are

$$\mathbf{V} = \mathbf{Z}_e \mathbf{I} + \mathbf{T}_{em} \mathbf{v} \quad (1)$$

$$\mathbf{F} = \mathbf{T}_{me} \mathbf{I} + \mathbf{z}_m \mathbf{v} \quad (2)$$

with voltage across the transducer terminals V , blocked electrical impedance Z_e , current through the transducer I , transducer output velocity v , transducer output force F , mechanical impedance of the transducer z_m , transduction coefficient (electrical from mechanical) T_{em} , and transduction coefficient (mechanical from electrical) T_{me} .

The force output from the transducer is assumed to act on a load of mechanical impedance z_L . Therefore equation 2 can be written

$$\mathbf{0} = \mathbf{T}_{me} \mathbf{I} + (\mathbf{z}_m + \mathbf{z}_L) \mathbf{v} \quad (3)$$

Solving for V/I in terms of the transduction coefficients and impedances results in

$$\mathbf{Z}_{ee} = \frac{\mathbf{V}}{\mathbf{I}} = \mathbf{Z}_e + \frac{(-\mathbf{T}_{em} \mathbf{T}_{me})}{\mathbf{z}_m + \mathbf{z}_L} = \mathbf{Z}_e + \mathbf{Z}_{mot} \quad (4)$$

Z_{ee} is the total electrical impedance of the system, which is the sum of the blocked electrical impedance Z_e , and the motional impedance term Z_{mot} . The blocked electrical impedance is defined as the impedance observed when the mechanical side is prevented from moving or "blocked". The motional impedance term represents the interaction of the electrical and mechanical sides of the transducer and thus it provides a measure of the performance of the transduction element, the Terfenol-D sample.

Figures 1, 2 and 3 show experimental data from the laboratory Terfenol-D this transducer. Tests were performed at 2.0 ksi prestress, with a drive level of 5 Oe, and a magnetic bias of 310 Oe. The magnitude and phase (bode plot) of the total

impedance Z_{ee} is plotted versus frequency in Figure 1; the real and imaginary components of Z_{ee} versus frequency are shown in Figure 2. The motional impedance term is seen in the Nyquist plot, Figure 3 as a circle, commonly referred to as the mobility loop. This mobility loop represents the z shaped resonance and anti-resonance (between 2.4 and 4.2 kHz) seen in the bode plot, Figure 1. Figure 3 also shows the point where the mobility loop crosses itself, labeled R_b and X_b . This point will be used to provide a measure of the magnetomechanical coupling discussed in section 5. If there is no transduction process taking place, the magnitude of Z_{ee} will collapse to the thin line shown in the magnitude of Figure 1. This can be considered the blocked impedance Z_e , discussed above. Assuming Z_e is relatively constant over the frequencies of the mobility loop (the slope of this line is 'slight'), the change in Z_e over the bandwidth of the mobility loop can be ignored. In this case all the information needed from Z_{mot} can be taken directly from the mobility loop in Z_{ee} . Otherwise Z_e must be subtracted from Z_{ee} before the above parameters can be measured from Z_{mot} . The maximum magnitude of the motional impedance function, the diameter of the mobility D_z , determines the impedance resonance f^R , see Figure 3.

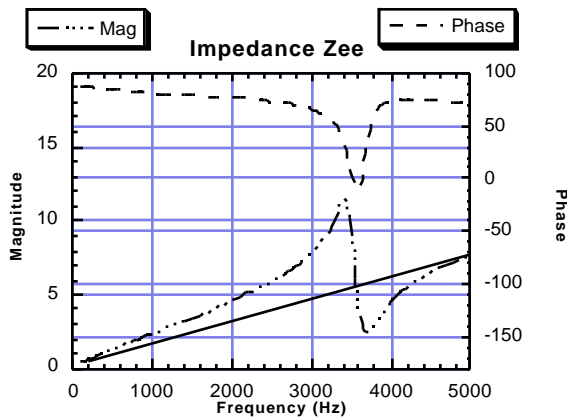


Figure 1. Impedance Bode Plot (Magnitude and phase) Terfenol-D transducer.

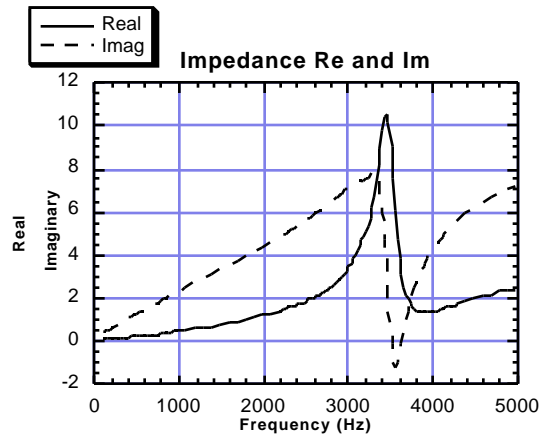


Figure 2. Impedance real and imaginary components.

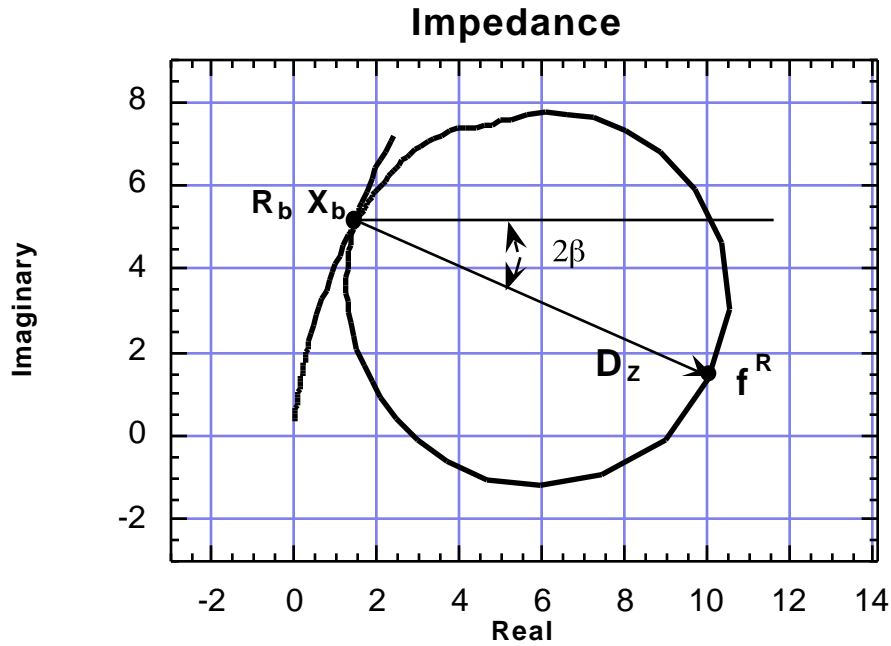


Figure 3. Vector-impedance locus from Terfenol-D transducer.

Note that this does not correspond to the peak in the magnitude of Z_{ee} . In general there is a phase shift or dip angle 2 associated with the mobility loop diameter D_z , as shown in Figure 3. Mathematically, this is due to the fact that the transduction coefficients (T_{em} and T_{me}) are vector operators; physically, this is explained by the dissipative effects inherent in the transduction process. The half power point frequencies, which will be needed to calculate the quality factor, are found at ± 90 degrees from the resonance on the mobility loop.

The total electrical admittance $Y_{ee} = I/V$, is the reciprocal of the total electrical impedance $Z_{ee} = V/I$. Graphically it is the geometric inversion of the total electrical impedance with respect to unity. The total electrical admittance Y_{ee} can be broken up into the blocked admittance term Y_e and the admittance mobility term Y_{mot} .

$$Y_{ee} = Y_e + Y_{mot} \quad (5)$$

It can be shown that Y_{mot} , which is not the reciprocal of Z_{mot} , is

$$Y_{mot} = \frac{(-T_{em}T_{me} / Z_e^2)}{z_m + z_L + (-T_{em}T_{me} / Z_e^2)} \quad (6)$$

These functions can then be analyzed the same as the impedance above. Figure 4 shows a bode plot of the admittance function, Figure 5 shows the admittance real and imaginary components versus frequency, and Figure 6 shows the vector-admittance real and imaginary loci.

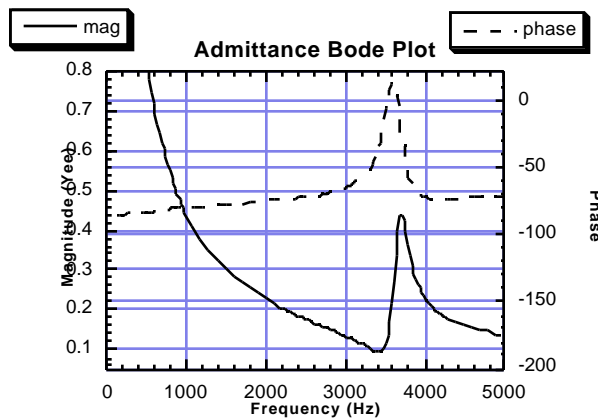


Figure 4. Admittance Bode Plot (Magnitude and phase) of a Terfenol-D transducer.

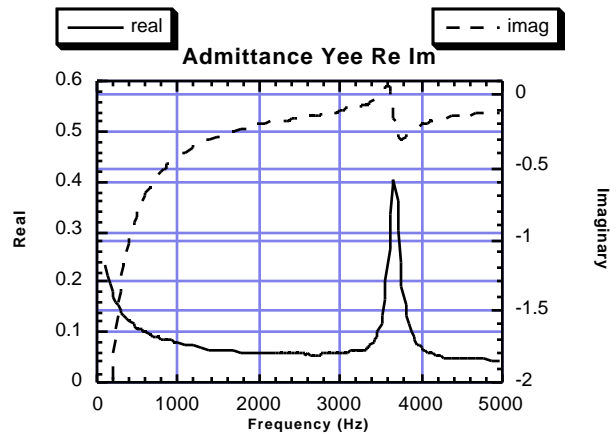


Figure 5. Admittance real and imaginary components.

The diameter of the admittance mobility loop D_Y , shown in Figure 6, determines the resonance f^A . The half power point frequencies for the admittance are found at ± 90 degrees from the resonance on the admittance mobility loop. Much information about the performance of the transducer and hence the Terfenol-D can be gained from an analysis of these figures.

The voltage V across the drive coil and current I entering and leaving the drive coil are available directly from the transducer. Therefore the complex electrical impedance V/I and admittance I/V can be calculated from these measurements. The pick-up coil, described above, provides a better measure of voltage; since it fits directly on the Terfenol-D rod there is less flux leakage associated with it than with the drive coil. The resonant frequency from the impedance f^R and the resonant frequency from the admittance f^A together provide the information needed to determine many of the material properties of Terfenol-D. For example, as described below, one measure of the effective magnetomechanical coupling figure of merit for the transducer can be found directly from these two resonant frequencies, f^R and f^A , shown in Figures 3 and 6 respectively. One of the often mentioned difficulties of using these resonant frequencies to determine material properties is the sensitivity of the frequency to the shape of the mobility loop. Very good quality circles are needed to accurately pick off the resonant frequency of interest. There are several reasons why an impedance or admittance mobility loop would not be circular in shape. First, spurious mechanical resonances due to transducer parts etc. can warp the shape of the circle; spurious resonances can even introduce additional circles inside the mobility loop. Second, variations from a true circle are expected in real life tests because of losses, due to hysteresis and eddy currents. These losses will tend to decrease the reactance, the imaginary component of the impedance, resulting in a more oval shape.

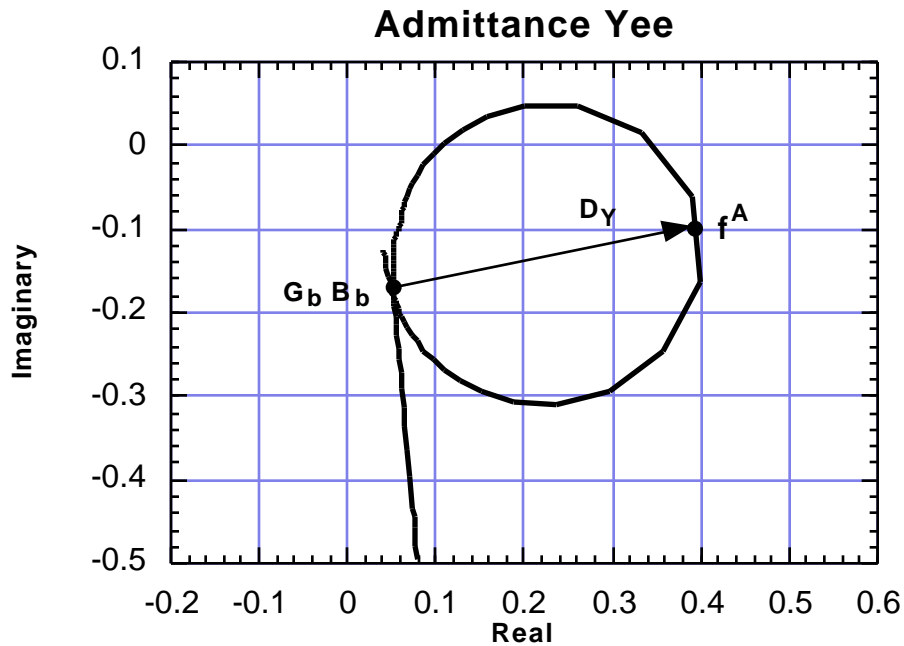


Figure 6. Vector-admittance locus from Terfenol-D transducer.

3. MAGNETOSTRICTIVE MODEL

The coupling between the mechanical strain and the magnetization of the material is captured by the low signal linear magnetostrictive equations given below

$$\varepsilon = \sigma/E^H + q H \quad (7)$$

$$B = q \sigma + \mu^{\sigma} H \quad (8)$$

with strain ε , stress σ , Young's modulus at constant applied magnetic field strength E^H , linear coupling coefficient q , magnetic permeability at a constant stress μ^{σ} , applied magnetic field strength H , and magnetic flux density B within the Terfenol-D. The source of this equation is the linearization of the differential response of the strain ε and B to changes in only two factors, the applied field H and stress σ . Several important assumptions are built into these magnetostrictive equations. First, linear operation of the transducer is assumed. Although the magnetostrictive effect is nonlinear, for low signal levels, less than one-third the maximum strain capability³, the linear equations of magnetostriction provide a good first approximation. Second, the magnetostriction process is assumed to be reversible according to

$$\left. \frac{dB}{d\sigma} \right|_H = \left. \frac{d\varepsilon}{dH} \right|_\sigma = q \quad (9)$$

where H is held constant for the first derivative and σ is held constant for the second. These two assumptions lead to a simplification of the strain coefficient q shown in equations 7 and 8. Hysteresis evidenced in strain versus applied field plots proves this to be a poor assumption, however it provides a starting point for material property analysis. Finally, strain and stress along the length of the sample are assumed to be uniform.

Clearly the interplay between the mechanical and magnetic effects is important. Magnetic domain wall motion and hence mechanical strain is produced by both mechanical stress and by applied magnetic fields. Similarly, the magnetic induction B will respond to the applied field H, as well as the mechanical stress. A first look at these equations tells much about the response of the material and the performance of a magnetostrictive transducer to external conditions. Increasing H will increase the strain output for a fixed prestress; similarly increasing the stress, which is compressive or negative in the equation, will decrease the strain for a fixed applied field. Magnetic induction B will increase with applied field H (or increased permeability) when the stress is kept constant and with decreasing (less compressive) stress when the applied field is kept constant.

4. MECHANICAL MODEL OF THE TRANSDUCER

A mechanical model of the transducer can be formulated using spring, mass, and damper lumped parameter components. The transducer was designed with a seismic base mass, sufficiently massive to simulate a fixed boundary at one end of the magnetostrictive rod. This means that all points in the rod move relative to the fixed end, allowing "single output" behavior. The rod can then be modeled as a linear spring element. In addition, great care was taken in the design, construction, and assembly of the transducer to ensure clean circular mobility loops. As described above, a circular mobility loop is required to obtain an accurate measure of the resonant and half power point frequencies. Any errors in the estimation of these frequencies will introduce errors in the material properties. Spurious resonances are the most common source of deviations in the mobility loop. Reducing the mass of internal parts increases the frequency of the spurious resonances associated with these parts, thus effectively increasing the operating bandwidth. Due to the small displacements, tolerances in the transducer had to be minimized. Finally design considerations must make it possible to consistently and accurately apply a calibrated prestress to the sample.

5 MATERIAL PROPERTY CALCULATIONS

The magnetostrictive equations, transduction equations, and the mechanical model of the transducer, are used to calculate the material properties from swept sine transducer measurements as described in detail by Hall³. The electrical impedance and admittance mobility loops are used to determine the resonant, anti-resonant, and half power point frequencies. The rest of the material properties can then be calculated using these frequencies and readily measurable transducer and Terfenol-D rod parameters as follows.

Quality factor Q is given by

$$Q = \frac{f^*}{f_2 - f_1} \quad (10)$$

where f^* is the resonant frequency of the transducer measured from either the electrical impedance or admittance mobility loop; f_2 and f_1 are the one-half power points. The quality factor provides a measure of the damping in the system. The larger the quality factor the lower the damping in the system.

The linear rod stiffness, k_m^H , is given by

$$k_m^H = (2\pi f^R)^2 m_1 m_2 / (m_1 + m_2) - k_{mps} \quad (11)$$

with the stiffness of the transducer prestress mechanism k_{mps} , mass of the transducer base m_1 , and the effective dynamic mass of the Terfenol-D rod and any external load m_2 .

Axial strain coefficient q , also known as the linear coupling coefficient is

$$q = \frac{\varepsilon}{H} \left[1 + \frac{k_{mps}}{k_m^H} \right] \quad (12)$$

The strain ε is calculated from the displacement at the free end of the rod, the measured acceleration divided by the squared circular frequency, and the length of the rod. Graphically, q can be seen as the local slope of the strain versus applied field plot (often called the hysteresis or butterfly curve) for a given constant stress. In general, values for q are calculated from ε/H at low frequency, since the tilt of the minor hysteresis loops can change considerably with frequency.

Magnetomechanical coupling k^2 is the energy conversion efficiency; it represents the fraction of magnetic energy that can be converted to mechanical energy per cycle and vice versa. k^2 is always between 0 and 1; a perfect energy converter would have a coupling of 1. Hall derives equation 13 for the magnetomechanical coupling of the Terfenol-D alone.

$$k^2 = \frac{k_{eff}^2 (k_m^2 + k_{mps})}{k_m^2 \left[k_m^H + \frac{k_{eff}^2 k_{mps}}{k_m^2} \right]} \quad (13)$$

The effective magnetomechanical coupling is calculated from the measured resonant and anti-resonant frequencies as

$$k_{eff}^2 = 1 - (f^R/f^A)^2 \quad (14)$$

where k_m^2 is the flux leakage measured for the transducer in use. This is known as the dynamic method of calculating the magnetomechanical coupling factor (as opposed to the “three parameter method” which calculates this coupling factor by setting $k^2 = q^2 E^H / \mu$). Other graphical methods of calculating the coupling are available from the theory of electroacoustics. Given the vector impedance loci, k_{eff}^2 can be found from the diameter of the circle D_z , the imaginary component of the crossover point X_b , and the quality factor Q_z .

$$k_{eff}^2 = \frac{1}{1 + X_b Q_z / D_z} \quad (15)$$

A similar expression can be derived from the vector admittance loci, where D_y is the diameter of the circle, B_b is the imaginary component of the crossover point, and Q_y is the quality factor.

$$k_{eff}^2 = \frac{D_y}{B_b Q_y} \quad (16)$$

According to Savage⁴ k_{eff}^2 from the impedance mobility loop provides reliable results, while k_{eff}^2 from the admittance does not.

There are two Young’s moduli that need to be considered for a magnetostrictive material. E^H is the Young’s modulus at constant applied field and E^B is the Young’s modulus at constant magnetic flux density in the material. For a Terfenol-D rod of length L and area A :

$$E^H = k_m^H L / A \quad (17)$$

The relation between the two moduli is determined by the magnetomechanical coupling,

$$\mathbf{E}^{\mathbf{H}} = \mathbf{E}^{\mathbf{B}} (1 - k^2) \quad (18)$$

Since k^2 can never be greater than one, it is clear that $\mathbf{E}^{\mathbf{B}}$ is larger than $\mathbf{E}^{\mathbf{H}}$, that is the Terfenol-D rod appears stiffer at constant B than at constant H. Physically, this follows from the implication of constant B preventing magnetic domain rotations and hence increasing a rod's stiffness relative to behavior at constant H.

The magnetic permeability μ is the slope of the B versus H plot ($B = \mu H$). Again there are two magnetic permeabilities to consider and they are related by the magnetoelastic coupling factor. At a constant stress the permeability μ^σ can be found from

$$\mu^\sigma = q^2 \mathbf{E}^{\mathbf{H}} / k^2 \quad (19)$$

This is known as the three parameter method, which relies on several assumptions. First the parameters q^2 , $\mathbf{E}^{\mathbf{H}}$, and k^2 must be measured under the same conditions, for example at the same frequency, or loading conditions. Additionally this formulation assumes that $d|dB|_H$ and $d|dH|$ are both equal to q ; an assumption which is only true if the magnetostriction is reversible which it is known not to be. A more accurate measure of the permeability of the material at constant stress is given by the differential form

$$\mu^\sigma = \frac{dB}{dH} \quad (20)$$

which is a complex function. In terms of the measurable quantities, V voltage measured by a pick-up coil of N_{pu} turns and area A_{pu} , the current I through the drive coil of n turns per unit length, of the transducer,

$$\mu^\sigma = \frac{V}{N_{pu} A_{pu} I n (-j\omega)} \quad (21)$$

where j represents a 90 degree phase shift in the frequency domain, resulting from the induced voltage V being proportional to the time derivative of B (Faraday's law of electromagnetic induction). The permeability will be a function of frequency, reaching a peak around the electrical impedance (V/I) resonance. Since eddy current losses are related to the permeability, this has important implications for maximum efficiency operation. Once μ^σ and k^2 are known the permeability at constant strain μ^ϵ can be found from

$$\mu^\epsilon = \mu^\sigma (1 - k^2) \quad (22)$$

The difference between these two permeabilities can be understood by considering the rotation of the magnetic domains. The rotation of the magnetic domains increases magnetic flux density B within the Terfenol-D rod. At a constant strain the rod is essentially blocked and the magnetic domains are not allowed to rotate. In contrast to this case, under constant stress the magnetic domains are allowed to rotate. Therefore for a given applied field H, B and hence slope μ will be larger for the constant stress case than for the constant strain case.

The speed of a wave through the material is directly proportional to the square root of the Young's Modulus over the density of the material. Again, there will be two speeds of sound $c^{\mathbf{H}}$ and $c^{\mathbf{B}}$ coming from the two Young's Moduli $\mathbf{E}^{\mathbf{H}}$ and $\mathbf{E}^{\mathbf{B}}$, one at constant H and one at constant B.

$$c^{\mathbf{H}} = \sqrt{\frac{\mathbf{E}^{\mathbf{H}}}{\rho}} \quad (23)$$

$$c^{\mathbf{B}} = \sqrt{\frac{\mathbf{E}^{\mathbf{B}}}{\rho}} \quad (24)$$

6. TRENDS IN MATERIAL PROPERTIES

The importance of accurately identifying all the operating conditions of a given test cannot be overstated. Terfenol-D has material properties which are quite dependent on operating conditions. This is to say that the performance of a sample depends on the state of the material which in turn is inextricably linked to the operating conditions.

Several examples of trends in the material properties for changes in operating conditions are presented below. In the following discussion, all operating conditions are kept constant except the ones mentioned as being changed. Experimental data will be examined to help elucidate the nature of the equations for the material properties. The laboratory transducer described above was tested at different drive levels, with different prestresses; other controllable testing conditions, such as load, and temperature, and magnetic bias point, were kept the same in all tests. Figures 7 and 8 shows magnitude (bottom with scale on the left) and phase (top with scale on the left) versus frequency from several tests.

Material property trends due to changing the drive level, the amplitude of the input current to the drive coil, show complex behavior. Hall³ provided experimental evidence and simulations that show k^2 increasing as drive level increases. This is explained by equation 1, where k^2 is one minus the square of the ratio of f^R to f^A . For graphical purposes the trend in f^R and f^A can be traced by following the trend in the impedance resonance and anti-resonance respectively. Figure 7 shows that this difference in the frequency (the gap between the resonance and anti-resonance) increases with increasing drive level. In addition, f^R (note the resonance peak in Figure 7) shifts to the left, to lower frequencies, with increasing drive level. This in turn means that the Young's Moduli (equations 17 and 18) and speeds of sound (equations 23 and 24) will be decreasing with drive level.

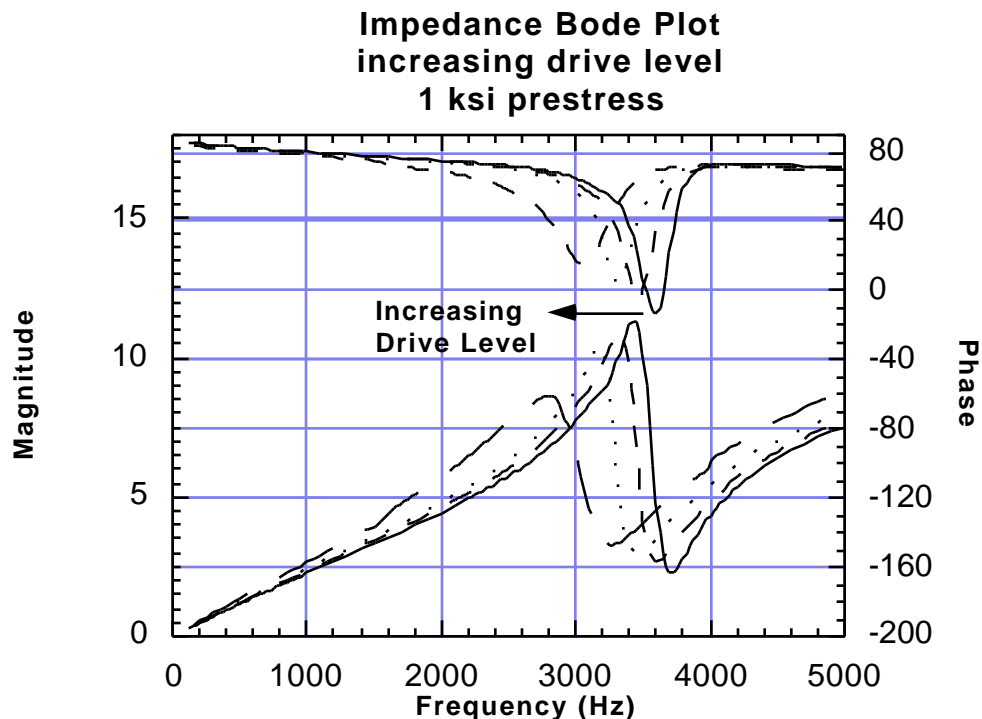


Figure 7. Impedance magnitude and phase at 1.0 ksi prestress. As the drive level increases, the resonant frequency shifts left, to a lower frequency, while the magnitude decreases.

Data taken under the same conditions, changing only the prestress from 1.0 ksi to 2.0 ksi, shows an interesting trend. Figure 8 shows the results from 2.0 ksi prestress cases at two drive levels, 5 and 50 Oe. The peak of the resonance noticeably increases from the low to high drive level. Hall's simulations and experimental data support this trend. However, this trend is not seen in the 1.0 ksi tests shown in Figure 7. Here the magnitude of the impedance resonance actually decreases significantly as drive level increases. Other trends in the material properties remain the same with increasing drive level for tests at both prestresses, f^R decreases, and Young's Moduli and speed of sound decrease. While this trend indicates that damping is appreciable for the lower prestress levels and less important at higher prestress, it's full significance has not been explored. However, it does highlight the point that the operating conditions for a Terfenol-D transducer interact in often surprising ways and great care must be taken to ensure proper conditions are maintained during testing or operation.

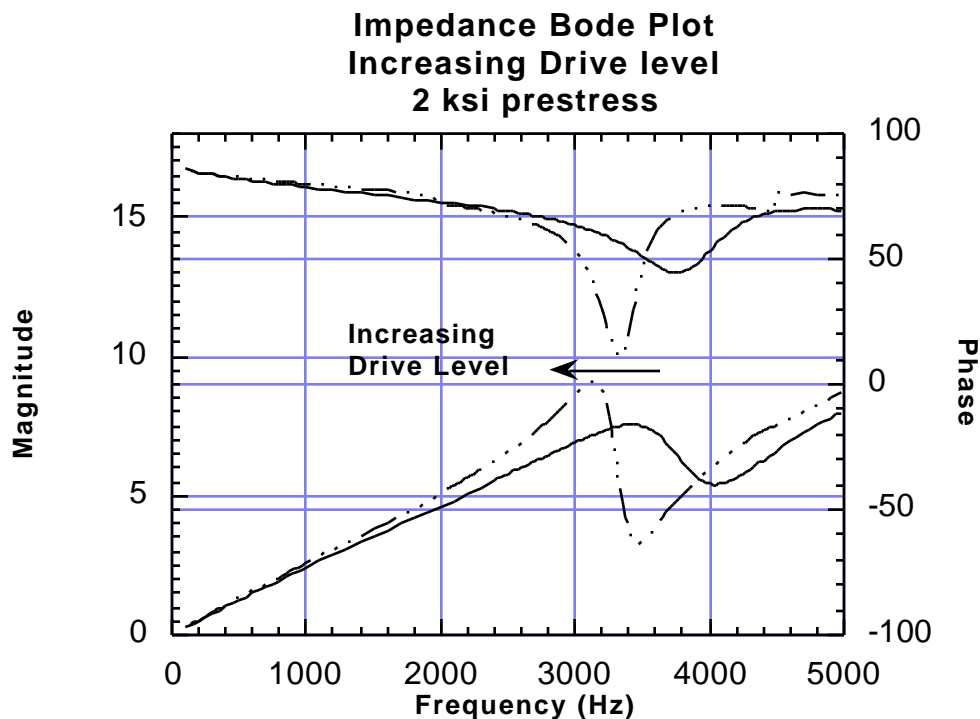


Figure 8. Impedance magnitude and phase at 2.0 ksi prestress. As the drive level increases, the resonant frequency shifts left, to a lower frequency, while the magnitude increases.

7. CONCLUSIONS

Procedures for obtaining Terfenol-D material properties from transducer measurements are presented. The equations for the material properties of interest, such as Young's moduli, permeabilities, magnetomechanical coupling factor, and the axial strain coefficient, are compiled from electroacoustic's model of transduction, a magnetostrictive model, and a mechanical model of the transducer. The properties are discussed and trends from experimental data are shown. The operating conditions are found to be of particular concern given the sensitivity of the Terfenol-D material properties to these conditions.

8. ACKNOWLEDGMENTS

We would like to acknowledge the financial support of the NASA Graduate Student Research Program at the Langley Research Center (Dr. Richard Silcox technical advisor), and the NSF Young Investigator Award (Dynamic Systems and Controls Division). Inspiration from Dr. David Hall through many lively discussions has been greatly appreciated.

9. REFERENCES

- 1 M.B. Moffet, A.E. Clark, M. Wun-Fogle, J. Linberg, J.P. Teter, E.A. McLaughlin. "Characterization of Terfenol-D for magnetostrictive transducers," J.Acoust.Soc.Am. 89 (3), March, 1991.
- 2 F.V. Hunt, "Electroacoustics: The Analysis of Transduction, and its Historical Background," American Institute of Physics for the Acoustical Society of America, 1982.
3. D.L. Hall, "Dynamics and vibrations of magnetostrictive transducers.," Ph.D. Dissertation, Iowa State University 1994.
4. H.T. Savage, A.E. Clark, and J.H. Powers. "Magnetomechanical coupling and E effect in highly magnetostrictive rare earth - Fe₂ Compounds.," IEEE Transactions on Magnetics, vol. Mag-11, no. 5, September, 1975.